hydrolysis with solvent H_2O, is consistent with the inverse deuterium isotope effect,[22] with the lack of general acid catalysis, and with the apparent activation parameters.

Acknowledgment. J.N.C. expresses appreciation to the donors of the Petroleum Research Fund, administered by the American Chemical Society, for partial support of this work and to E. J. Mastascusa for assistance in implementing the Runge–Kutta routines.

(22) Bunton, C. A.; Shiner, V. J., Jr. *J. Am. Chem. Soc.* **1961**, *83*, 3214.

Registry No. $[(en)_2Co(OH_2)(S_2O_3)]^+$, 86900-35-8; *trans*-$[(en)_2Co(OH_2)(S_2O_3)]^+$, 62656-34-2; *cis*-$[(en)_2Co(OH_2)(S_2O_3)]^+$, 86900-36-9; *trans*-$[(en)_2Co(Cl)(S_2O_3)]$, 86853-85-2; *trans*-$[(en)_2Co(NCO)(S_2O_3)]$, 86853-86-3; *trans*-$[(en)_2Co(Cl)_2]Cl$, 14040-33-6; $Na[trans\text{-}[(en)_2Co(C_2O_4)(S_2O_3)]]$, 86853-87-4; *trans*-$[(en)_2Co(S_2O_3)_2]^-$, 62529-95-7; iodine, 7553-56-2.

Contribution from the Department of Chemistry and Biochemistry, Utah State University, Logan, Utah 84322, Department of Chemistry, University of Arizona, Tucson, Arizona 84721, and Fakultät für Biologie, Universität Konstanz, D-7500 Konstanz, West Germany

Molybdenum(V) and -(VI) Complexes with Deprotonated Aromatic Amino Ligands

O. A. RAJAN,[1a] J. T. SPENCE,*[1a] C. LEMAN,[1a] M. MINELLI,[1b] M. SATO,[1b] J. H. ENEMARK,[1b] P. M. H. KRONECK,[1c] and K. SULGER[1c]

Received April 21, 1983

Reaction of $MoO_2(acac)_2$ or MoO_2Cl_2 with tridentate (NOS, NO_2) ligands having aromatic amino groups gives MoL_2 (L = *N*-(2-hydroxybenzyl)-2-mercaptoaniline, *N*-(2-hydroxybenzyl)-2-hydroxyaniline) complexes in which both oxo groups have been displaced and the amino groups deprotonated. The complexes exhibit reversible electrochemical behavior involving $MoL_2/MoL_2^-/MoL_2^{2-}$ complexes. The Mo(V) complex $[Et_4N][MoL_2]$ (L = *N*-(2-hydroxybenzyl)-2-mercaptoaniline) has also been prepared and its structure determined. It has highly distorted octahedral geometry with short Mo–N bonds. The oxygen analogue has been obtained in solution by electrochemical reduction of the corresponding Mo(VI) complex. The EPR parameters of the Mo(V) complexes obtained by computer simulation are reported. Reaction of *N,N'*-bis(2-hydroxybenzyl)-*o*-phenylenediamine and 1,2-bis(2-hydroxyanilino)ethane with $MoO_2(acac)_2$ gives complexes of formula $MoO_2(LH_2)$. One-electron electrochemical reduction gives monomeric Mo(V) complexes, in which the amino ligands are most probably deprotonated. The Mo(V)–oxo complexes are similar in properties to previously reported Mo(V)–oxo complexes with deprotonated tetradentate aromatic N_2S_2 ligands. Their EPR spectra show well-resolved ^{14}N shfs from two equivalent nitrogens. They are reversibly reduced electrochemically in a one-electron step to Mo(IV) species and oxidized irreversibly to $MoO_2(LH_2)$. The generation of the stable Mo(V) intermediates in the electrochemical reduction of the Mo(VI) complexes mimics the redox behavior of molybdenum hydroxylases.

Introduction

The ability of transition metals in high oxidation states to deprotonate coordinated amino ligands is well-known,[2-4] and molybdenum(V) and -(VI) complexes with *o*-aminobenzenethiol having deprotonated amino (amido) groups have been reported.[5,6] Deprotonation of coordinated amino groups may be of importance with respect to molybdenum enzymes, for which coupled proton/electron-transfer processes have been postulated.[7]

Recently we reported preliminary results for two Mo(V)–oxo complexes, $[Et_4N][MoOL]$, where L^{4-} is a tetradentate aromatic amino thiol ligand with an N_2S_2 donor set in which the amino groups are deprotonated.[8] We report here the detailed syntheses and the EPR parameters of these complexes, the syntheses and properties of two new non-oxo Mo(VI) complexes and one new non-oxo Mo(V) complex having deprotonated amino ligands, and the X-ray crystal structure of the latter. In addition, the syntheses and electrochemical behavior of two new Mo(VI)–dioxo complexes with normal (i.e., protonated) amino ligands and the solution properties of three Mo(V) complexes with deprotonated amino ligands,

Table I. Electrochemical Data

complex	Mo(VI)/Mo(V) $E_{1/2}$[a]	Mo(VI)/Mo(V) n[b]	Mo(V)/Mo(IV) $E_{1/2}$[a]	Mo(V)/Mo(IV) n[b]
$Mo(hbma)_2$[d]	−0.02	0.92	−1.15	1[c]
$Mo(hbha)_2$[d]	−0.26	1.04	−1.36	1[c]
$MoO_2(haeH_2)$[e]	−1.41[g] −0.02[h]	1.01	−1.70	1[c]
$MoO_2(hbpdH_2)$[f]	−1.41[g] −0.19[h]	1.04	−1.69	1[c]
$MoO_2(maeH_2)$[e]	−1.03[j] 0.14[h]	2.00[j]	−1.00[i]	1.05[i]
$MoO_2(mabH_2)$[e]	−1.09[j] 0.19[h]	2.05[j]	−1.02[i]	1.10[i]

[a] $(E_{pc} + E_{pa})/2$ vs. SCE; 0.100 V/s scan rate. [b] Electrons/molecule. [c] Estimated by comparison of peak with peak of first reduction. [d] CH_2Cl_2, 0.10 M $[n\text{-}Bu_4N][BF_4]$. [e] DMF, 0.10 M $[Et_4N]Cl$. [f] MeCN, 0.10 M $[Et_4N]Cl$. [g] Irreversible reduction. [h] Irreversible oxidation. [i] $[Et_4N][MoO(mae)]$ and $[Et_4N][MoO(mab)]$, respectively.[8] [j] Reduction from Mo(VI) to Mo(IV).[5]

(1) (a) Utah State University. (b) University of Arizona. (c) Universität Konstanz.
(2) Balch, A. L.; Holm, R. H. *J. Am. Chem. Soc.* **1966**, *88*, 5201.
(3) Stiefel, E. I.; Waters, J. H.; Billig, E.; Gray, H. B. *J. Am. Chem. Soc.* **1965**, *87*, 3016.
(4) Balch, A. L.; Rohrsheid, F.; Holm, R. H. *J. Am. Chem. Soc.* **1965**, *87*, 2301.
(5) (a) Yamanouchi, K.; Enemark, J. H. *Inorg. Chem.* **1978**, *17*, 2911. (b) Gardner, J. K.; Pariyadath, N.; Corbin, J. L.; Stiefel, E. I. *Ibid.* **1978**, *17*, 897.
(6) (a) Yamanouchi, K.; Enemark, J. H. *Inorg. Chem.* **1978**, *17*, 1981. (b) Pariyadath, N.; Newton, W.; Stiefel, E. I. *J. Am. Chem. Soc.* **1976**, *98*, 5388.
(7) Stiefel, E. I. *Prog. Inorg. Chem.* **1976**, *22*, 1.
(8) Spence, J. T.; Minelli, M.; Kroneck, P. *J. Am. Chem. Soc.* **1980**, *102*, 4538.

0020-1669/83/1322-3065$01.50/0

Table II. EPR Data

complex	g_x[a]	g_y[a]	g_z[a]	g_0[b]	^{95,97}Mo, A_x[c]	A_y[c]	A_z[c]	A_0[b]	^{14}N, A
					$cm^{-1} \times 10^4$				$cm^{-1} \times 10^4$
$[Et_4N][Mo(hbma)_2]$[d]	1.9790	1.9790	1.9455	1.9690	22.0	22.0	60.0	39.0	
$[Mo(hbha)_2]^-$[e]	1.9240	1.9640	1.9875	1.9550	59.0	46.0	20.0	40.5	
$[MoO(hae)]^-$[f]	1.9550	1.9645	1.9795	1.9570	67.5	28.5	20.0	38.5	2.15[b]
$[MoO(hbpd)]^-$[e]	1.9685	1.9645	1.9505	1.9590	29.0	32.0	73.0	46.5	2.23[g]
$[Et_4N][MoO(mae)]$[a,h]	1.9740	1.9820	2.0025	1.9860	24.0	18.0	55.0	33.0	2.14[i]
$[Et_4N][MoO(mab)]$[a,h]	1.9730	1.9790	2.0040	1.9860	40.0	11.0	50.0	33.0	2.14[i]

[a] 77 K; ±0.0005 for g. [b] Room temperature. [c] 77 K; ±0.5 $cm^{-1} \times 10^4$ for A. [d] CH_2Cl_2. [e] MeCN. [f] DMF. [g] −5 °C. [h] Refined from previous values.[8] [i] −30 °C.

generated by electrochemical reduction of the corresponding Mo(VI) complexes, are described.

Results

Non-Oxo Mo(VI) Complexes. The ligands $hbmaH_3$[9] and $hbhaH_3$[9] react with $MoO_2(acac)_2$ to give non-oxo Mo(VI) complexes:

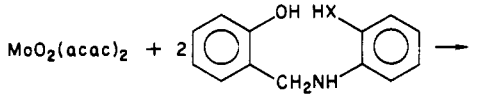

X = S: $hbmaH_3$
X = O: $hbhaH_3$

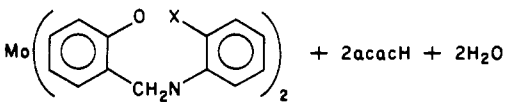

These complexes exhibit neither Mo=O nor N—H stretches in their IR spectra, and their analyses are in agreement with their formulation as indicated. Attempts to grow satisfactory crystals for X-ray structure determination have not been successful.

The electrochemistry of these complexes in aprotic solvents indicates they are reduced in two one-electron reversible steps, demonstrating their dithiolene-like character.[5b] The cyclic voltammograms of these complexes are identical with those of the corresponding Mo(V) complexes (Figure 1, Table I). $Mo(hbha)_2$ appears to be the first reported dithiolene-like Mo complex in which the donors are nitrogen and oxygen.[7]

Non-Oxo Mo(V) Complexes. The reaction of $hbmaH_3$ with $[Et_4N][MoO(SC_6H_4CH_3)_4]$ gives a non-oxo Mo(V) complex:

$$MoO(SC_6H_4CH_3)_4 + 2hbmaH_3 \rightarrow Mo(hbma)_2^- + 4HSC_6H_4CH_3 + H_2O$$

The complex was isolated as s the Et_4N^+ salt. Its IR spectrum has no Mo=O or N—H absorption bands, and its analysis is in agreement with its formulation as a non-oxo Mo(V) complex in which the ligand amino groups are deprotonated. Attempts to prepare the oxygen analogue $[Et_4N][Mo(hbha)_2]$ have not been successful. Both complexes, however, are generated quantitatively in solution by electrochemical reduction of the corresponding Mo(VI) complex. The formulation of the one-electron-reduction product of $Mo(hbma)_2$ as $[Mo(hbha)_2]^-$ is strongly suggested by a comparison of the cyclic voltammogram and electronic and EPR spectra of the electrochemically reduced solution with those of solutions of $[Et_4N][Mo(hbma)_2]$. In the case of $[Mo(hbha)_2]^-$, the cyclic voltammogram and electronic spectrum are basically similar to those of $[Et_4N][Mo(hbma)_2]$, with the differences (more negative reduction potentials, e.g.) reflecting the substitution of oxygen for sulfur (Table I).

(9) Ligand abbreviations: $hbmaH_3$, *N*-(2-hydroxybenzyl)-2-mercaptoaniline; $hbhaH_3$, *N*-(2-hydroxybenzyl)-2-hydroxyaniline; $haeH_4$, 1,2-bis(2-hydroxyanilino)ethane; $hbpdH_4$, *N,N'*-bis(2-hydroxybenzyl)-*o*-phenylenediamine; $maeH_4$, 1,2-bis(2-mercaptoanilino)ethane; $mabH_4$, 2,3-bis(2-mercaptoanilino)butane.

Table III. Crystallographic Data for $[NEt_4][Mo(hbma)_2]$

formula	$[NC_8H_{20}][Mo(OSNC_{13}H_{10})_2]$
fw	682.77
space group	*I2/a*
cell dimens	
a, Å	18.830 (15)
b, Å	17.437 (13)
c, Å	19.745 (15)
V, Å^3	6458.7 (85)
β, deg	94.989 (64)
Z	8
d_{obsd},[a] g/cm^3	1.392 (3)
d_{calcd}, g/cm^3	1.405
cryst shape	plate
cryst dimens, nm	0.37 × 0.15 × 0.13
radiation (Mo Kα), Å	0.71 073
data collection method	*θ*–2*θ* scan
scan speed, variable, deg/min	3.0–29.3
scan range, 2*θ*, deg	Mo $K\alpha_1$ − 1.0 to $K\alpha_2$ + 1.0
total background time/ peak scan time	0.5
2*θ* limit, deg	3.0–45.0
no. of unique data	4229
no. of data used in the calculations	2355, $I > 2\sigma(I)$
abs coeff, cm^{-1}	5.62

[a] The density was determined by the flotation method using a solution of carbon tetrachloride and hexane.

Table IV. Interatomic Distances (A) and Angles (deg) for $[Et_4N][Mo(hbma)_2]$

Mo-O1	2.030 (7)	Mo-O2	2.016 (8)
Mo-N1	2.043 (8)	Mo-N2	2.056 (9)
Mo-S1	2.363 (4)	Mo-S2	2.360 (4)
O1-Mo-O2	80.5 (4)	O2-Mo-N2	86.0 (3)
S1-Mo-S2	107.1 (2)	O2-Mo-S1	90.0 (3)
N1-Mo-N2	157.9 (3)	O2-Mo-S2	156.3 (2)
O1-Mo-N1	85.8 (3)	N1-Mo-S1	79.0 (3)
O1-Mo-N2	114.0 (3)	N1-Mo-S2	91.8 (3)
O1-Mo-S1	158.8 (3)	N2-Mo-S1	83.9 (3)
O1-Mo-S2	88.0 (3)	N2-Mo-S2	79.9 (3)
O2-Mo-N1	107.7 (3)		

$[Et_4N][Mo(hbma)_2]$ exhibits an axial EPR spectrum with $g_\perp$ ($g_x = g_y$) > $g_\parallel$ (g_z) and $A_\parallel$ (A_z) > $A_\perp$ ($A_x = A_y$) (Figure 4, Table II). In the case of $[Mo(hbha)_2]^-$, the EPR is rhombic with $g_z > g_y > g_x$ and $A_x > A_y > A_z$. Although superhyperfine splitting (shfs) by two equivalent ^{14}N atoms was expected, as reported for $[Et_4N][MoO(mab)]$ and $[Et_4N][MoO(mae)]$,[8,9] it was not detected over a temperature range from room temperature to 77 K.

The structure of $[EtN_4][Mo(hbma)_2]$ has been determined by X-ray crystallography (Figure 5). The molybdenum atom is six-coordinate, and the anion exhibits approximate C_2 symmetry. The complex is substantially distorted from meridional octahedral geometry, as evidenced by the pseudotrans angles, which are all less than 160° (Table IV). The overall coordination geometry is similar to that found for $Mo(NHC_6H_4S)_2(S_2CN(C_2H_5)_2)$,[6a] a related Mo(V) complex that also has approximate C_2 symmetry and deprotonated amino and

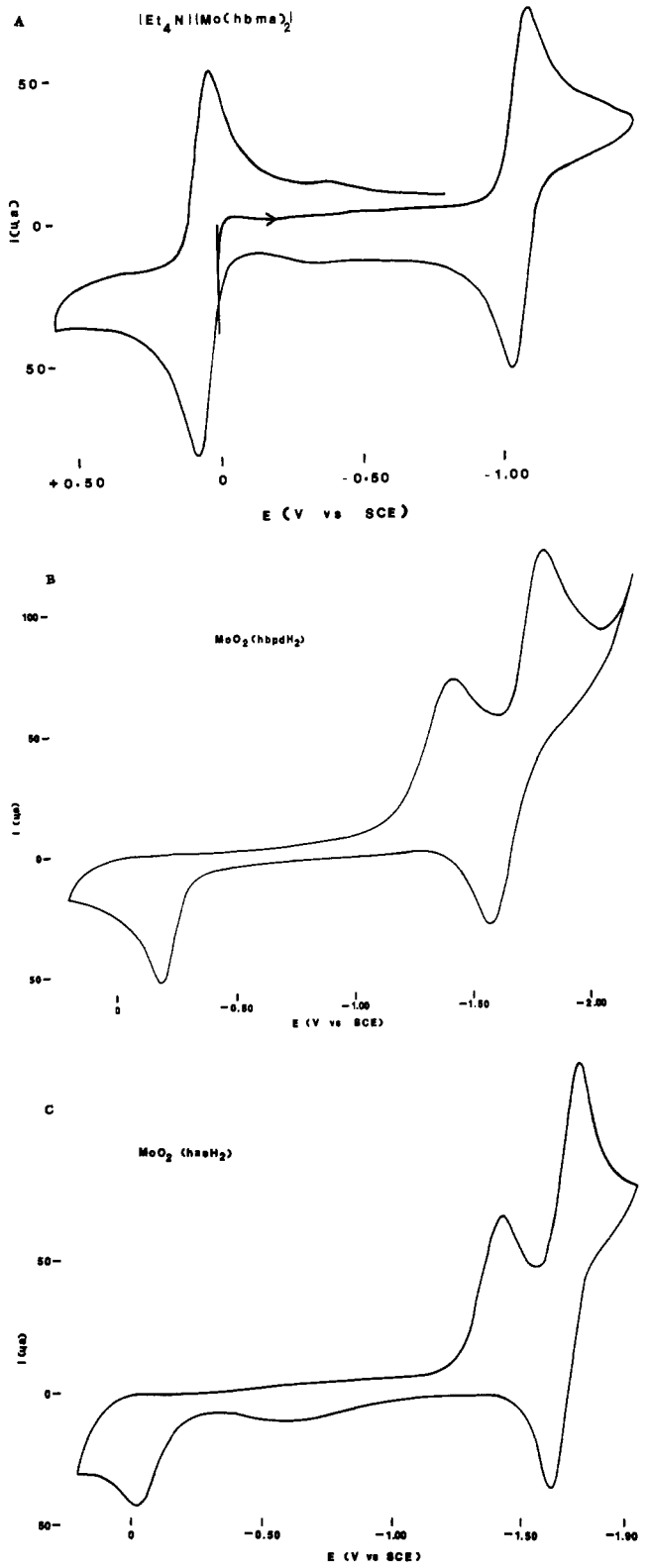

Figure 1. Cyclic voltammograms of complexes (5.00×10^{-4} M, 0.100 V/s): $[Et_4N][Mo(hbma)_2]$ and $MoO_2(hbpdH_2)$, CH_3CN, 0.10 M $[Et_4N]Cl$; $MoO_2(haeH_2)$, DMF, 0.10 M $[Et_4N]Cl$.

thiolate groups. The stereochemistry of the latter complex has been analyzed in detail and shown to be intermediate between an octahedron and a trigonal prism.[6a] Likewise, the structure of $[Mo(hbma)_2]^-$ can be viewed as an octahedron distorted toward a trigonal prism in which the two triangular faces contain atoms S1, O2, N2 and atoms S2, O1, N2, respectively (Figure 5).

The mean Mo–N distance (2.050 (9) Å, Table IV) is about 0.2 Å shorter than that observed for coordinated tetrahedral

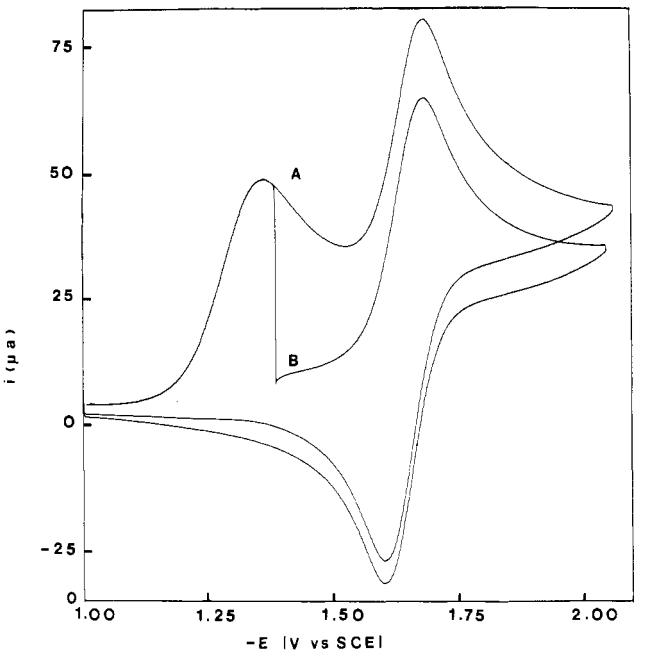

Figure 2. Cyclic voltammograms for $MoO_2(haeH_2)$ (9.20×10^{-4} M, DMF, 0.10 M $[Et_4N]Cl$, 0.100 V/s): (A) uninterrupted scan; (B) scan stopped at −1.385 V with current being allowed to decay to steady-state value, after which scan continued.

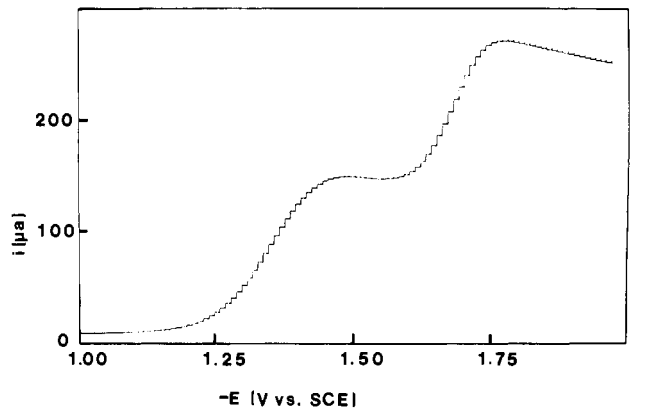

Figure 3. Pulse polarogram for $MoO_2(haeH_2)$ (9.20×10^{-4} M, DMF, 0.10 M $[Et_4N]Cl$, pulse inverval 5 s, 0.002 V/s).

nitrogen atoms.[10] There are two known structures with a deprotonated trigonal N atom coordinated to molybdenum in a high oxidation state (+5 and +6), $Mo(NHC_6H_4S)_2(S_2CN(C_2H_5)_2)$[6a] and $Mo(NHC_6H_4S)_3$.[5a] For $Mo(NHC_6H_4S)_2(S_2CN(C_2H_5)_2)$ the Mo–N distances are 2.001 (2) and 2.009 (2) Å; for $Mo(NHC_6H_4S)_3$ the mean Mo–N distance is 1.997 (8) Å. These short Mo–N distances are indicative of multiple bonding between the Mo atom and the trigonal, deprotonated N atom of the ligand. For comparison, in $MoOCl(thiooxine)_2$, which has neutral trigonal N atoms, the Mo–N distances are 2.210 (6) Å (N trans to Cl) and 2.408 (6) Å (N trans to the terminal oxo group).[11]

The mean Mo–S distance in $[Et_4N][Mo(hbma)_2]$ (2.362 (4) Å) is slightly shorter than those in other Mo(V) and Mo(VI) complexes of thiolate ligands. For $Mo(NHC_6H_4S)(S_2CN(C_2H_5)_2)$ the Mo–S distance to the NHC_4H_4S ligand is 2.384 (11) Å. In $Mo(NHC_6H_4S)_3$ the mean Mo–S distance is 2.418 (6) Å. The Mo–S distances in thiolate complexes of oxomolybdenum(V) and -(VI) are usually greater than 2.4 Å.[11-13] The Mo–O distance (Table IV) is about the same as

(10) Spivack, B.; Dori, Z. *Coord. Chem. Rev.* **1975**, *17*, 99.
(11) Yamanouchi, K.; Enemark, J. H. *Inorg. Chem.* **1979**, *18*, 1626.

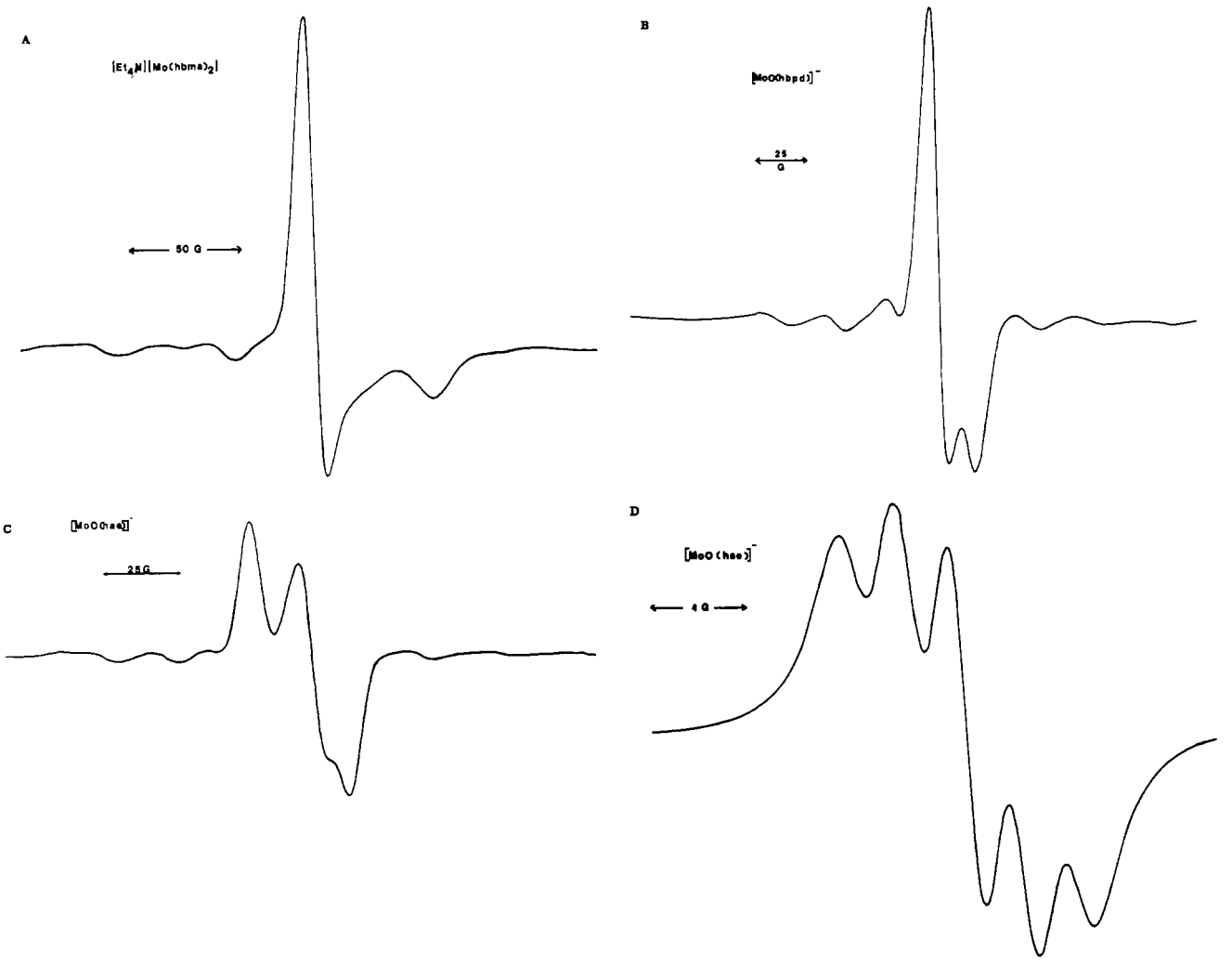

Figure 4. EPR spectra of complexes (77 K except as noted in Table II; 5.00×10^{-4} M): $[Et_4N][Mo(hbma)_2]$, CH_2Cl_2; $[MoO(hpbd)]^-$, CH_3CN; $[MoO(hae)]^-$, DMF.

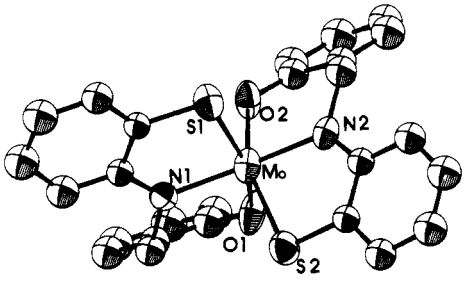

Figure 5. Perspective view of $[Mo(hbma)_2]^-$ along the approximate C_2 axis. Hydrogen atoms have been omitted for clarity. The geometry is approximately halfway between a meridonal octahedron and a trigonal prism in which the two trigonal faces contain atoms S1, O2, N2 and atoms S2, O1, N2, respectively.

reported for complexes of oxine ligands (2.030 (4) Å in $Mo_2O_3(oxine)_2(SCH_2CH_2O)$[14] and 2.039 (5) Å in $[H_2$–oxine$][MoOCl_3(oxine)]$).[15]

Mo(VI)–Dioxo Complexes. The ligands $hbpdH_4$ [9] and $haeH_4$ [9] react with $MoO_2(acac)_2$ to give dioxo complexes with normal (i.e., protonated) amino ligands, $MoO_2(hbpdH_2)$ and $MoO_2(haeH_2)$, as determined by analysis and IR and electronic spectra.

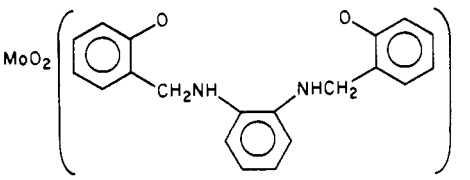

$MoO_2(hbpdH_2)$

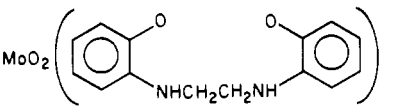

$MoO_2(haeH_2)$

The cyclic voltammograms of both complexes exhibit an irreversible one-electron-reduction peak at −1.41 V coupled to an oxidation peak at −0.19 V ($MoO_2(hbpdH_2)$) and −0.02 V ($MoO_2(haeH_2)$) (Figure 1, Table I). A second one-electron-reversible-reduction peak at −1.70 V is seen for $MoO_2(haeH_2)$ and a one-electron-quasi-reversible-reduction peak at −1.69 V for $MoO_2(hbpdH_2)$. One-electron coulometric reduction at −1.50 V for both complexes gives quantitative yields of monomeric Mo(V) complexes, as determined by EPR. Attempts to determine the number of electrons involved in the second reduction (−1.70 V) by coulometry failed due to high background currents. By stopping the CV scan for $MoO_2(LH_2)$ just beyond the first peak, allowing the current to decay

(12) Bruce, A.; Corbin, J. L.; Dahlstron, P. L.; Hyde, J. R., Minelli, M.; Stiefel, E. I.; Spence, J. T.; Zubieta, J. *Inorg. Chem.* **1982**, *21*, 917.
(13) Huneke, J. T.; Yamanouchi, K.; Enemark, J. H. *Inorg. Chem.* **1978**, *17*, 3695.
(14) Gelder, J. I.; Enemark, J. H.; Wolterman, G.; Boston, D. A.; Haight, G. P. *J. Am. Chem. Soc.* **1975**, *97*, 1616.
(15) Yamanouchi, K.; Huneke, J. T.; Enemark, J. H.; Taylor, R. D.; Spence, J. T. *Acta Crystallogr., Sect. B* **1979**, *B35*, 2326.

to a small value, and then resuming the scan, we established the base line for the second peak (Figure 2). This method allows a direct comparison of peak heights[16a] and indicates the second peak is most likely also a one-electron process. The normal-pulse polarogram (Figure 3) also indicates the two reductions involve the same number of electrons. The differential-pulse polarogram (DPP) for the second peak has a width at half-height ($W_{1/2}$) of 100 mV; the limiting value of $W_{1/2}$ for a one-electron reversible process as ΔE (pulse amplitude) approaches zero is 90.4 mV.[16b] After one-electron coulometric reduction at −1.50 V, $E_{1/2}$ for the second peak remains unchanged, and peak height agrees well with that determined by the method described above for determining the base line for the second peak. It therefore seems reasonably certain the second reduction is a one-electron process producing an Mo(IV) species.

The EPR spectrum of $[MoO(hae)]^-$ is similar in appearance to the EPR spectra of $[Et_4N][MoO(mab)]$ and $[Et_4N][MoO(mae)]$.[8] As expected, substitution of oxygen for sulfur in the ligands gives lower g values and slightly larger A values (Table II). With $[MoO(hae)]^-$, $A_x > A_y > A_z$, while this order is reversed for the N_2S_2 complexes. With $[MoO(hbpd)]^-$, $g_x > g_y > g_z$, while the N_2S_2 complexes have the more usually observed order, $g_z > g_y > g_x$ (Table II). With both $[MoO(hae)]^-$ and $[MoO(hbpd)]^-$, shfs of $\sim 2 \times 10^{-4}$ cm^{-1}, resulting from coupling of two equivalent ^{14}N nuclei to Mo(V), is observed. Similar coupling was found for $[Et_4N][MoO(mae)]$ and $[Et_4N][MoO(mab)]$[8] (Table II, Figure 4).

Discussion

The electrochemical results indicate the non-oxo complexes with $hbma^{3-}$ and $hbha^{3-}$ form a reversible electron-transfer series involving the +6, +5, and +4 states, demonstrating their dithiolene-like character:

$$Mo^{VI}(hbma)_2 \underset{-e^-}{\overset{e^-}{\rightleftharpoons}} Mo^{V}(hbma)_2^- \underset{-e^-}{\overset{e^-}{\rightleftharpoons}} Mo^{IV}(hbma)_2^{2-}$$

The electrochemistry of the Mo(VI)–dioxo complexes with $maeH_2^{2-}$ and $mabH_2^{2-}$ and the Mo(V)–oxo complexes with mae^{4-} and mab^{4-} indicates the Mo(VI)–dioxo complexes are irreversibly reduced to the Mo(V)–oxo complexes.[8] The Mo(VI)–dioxo complexes with $haeH_2^{2-}$ and $hbpd_2^{2-}$ are most probably reduced to Mo(V)–oxo species with deprotonated amino ligands, $MoOL^-$; this is based on a comparison of their solution properties (CV and electronic and EPR spectra) with those of the corresponding sulfur complexes, $[Et_4N][MoO(mae)]$ and $[Et_4N][MoO(mab)]$ (which have been shown to be identical in solution with the one-electron-reduction products of their Mo(VI)–dioxo complexes, $MoO_2(LH_2)$). In both cases, intensely colored 100% monomeric species, stable to NO_3^-, for which the EPR signal is split by two equivalent ^{14}N, are obtained. In both cases, the cyclic voltammograms of the solutions show reversible or quasi-reversible one-electron reductions and irreversible one-electron oxidations. In both cases, reoxidation by one electron gives the original $Mo^{VI}O_2(LH_2)$ complex. The Mo(V) complexes are further reversibly reduced, most likely to Mo(IV)–oxo complexes:

$$Mo^{VI}O_2(LH_2) \xrightarrow{e^-} Mo^{V}OL^- \underset{-e^-}{\overset{e^-}{\rightleftharpoons}} Mo^{IV}OL^{2-}$$

In the case of $MoO_2(maeH_2)$ and $MoO_2(mabH_2)$, the two reduction peaks are not separated; coulometric reduction by one electron, however, produces Mo(V)–oxo complexes quantitatively.[8] With $MoO_2(hbpdH_2)$ and $MoO_2(haeH_2)$, the two reductions are clearly separated (~0.30 V). These are among the few reported Mo(VI)–dioxo complexes that are electrochemically reducible to stable monomeric Mo(V)–oxo complexes[17] (reduction generally gives EPR-silent oxo-bridged Mo(V) dimers), and in this regard they mimic the redox behavior of the Mo enzymes xanthine oxidase and sulfite oxidase.[18] This behavior appears to be a result of the deprotonation of the amino groups with elimination of H_2O upon reduction:[8]

$$MoO_2(LH_2) \xrightarrow{e^-} MoOL^- + H_2O$$

The irreversibility of this step probably arises from the rearrangement of the coordination sphere accompanying oxo loss. The reversibility of the second reduction to the +4 state suggests a Mo(IV)–oxo complex with deprotonated ligands is formed. Attempts to synthesize such Mo(IV) complexes have been unsuccessful.[19]

The stability of the Mo(V)–oxo complexes with respect to dimerization probably is a result of the strong σ- and π-donor ability of the amido group and the imposition of a planar structure on the ligand when trigonal nitrogen replaces tetrahedral nitrogen:[8]

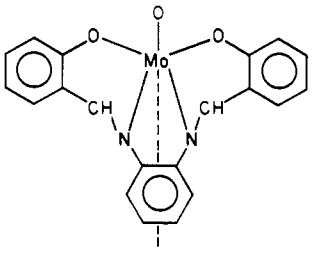

[MoO(hbpd)]$^-$

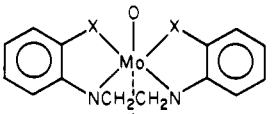

X = S: $[MoO(mae)]^-$
X = O: $[MoO(hae)]^-$

Briding through a cis position is thus prevented, while briding through a trans position is highly unfavorable because of the trans effect of oxo.[7] This is substantiated by the lack of reactivity of these complexes with NO_3^-,[8] which requires bonding of the NO_3^- at a cis position for electron transfer to occur.[20]

For most Mo(V)–oxo complexes, EPR data indicate the largest coupling constant is A_z, with the z axis along the Mo–oxo bond direction.[21] For the non-oxo species, it is not clear which axis should be designated as z (or $\perp$ for $[Et_4N][Mo(hbma)_2]$). The lack of ^{14}N shfs in these two complexes is in marked contrast to the EPR results for $Mo(NHC_6H_4S)_2(S_2CN(C_2H_5)_2)$, which has similar stereochemistry (vide supra) but shows a ^{14}N shfs of 2.2×10^{-4} cm^{-1}, with the unpaired electron being in the plane normal to the C_2 axis (**1**). The lack of ^{14}N shfs for $[Mo(hbma)_2]^-$ suggests that the

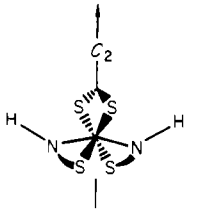

1

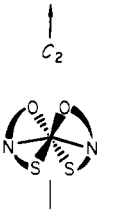

2

unpaired electron is an orbital that lies along the C_2 axis (**2**)

(16) (a) Bard, A. J.; Faulkner, L. R. "Electrochemical Methods. Fundamentals and Applications"; Wiley: New York, 1980; pp 233–234. (b) *Ibid.*, p 195.

(17) Charney, L. M.; Finklea, H. O.; Schultz, F. A. *Inorg. Chem.* **1982**, *21*, 549.

(18) Bray, R. C. *Adv. Enzmol. Relat. Areas* **1980**, *51*, 107; "Biological Magnetic Resonance"; Berliner, L. G., Reuben, J., Eds.; Plenum Press: New York, 1980; Vol. 2, p 45.

(19) Boyd, I. W.; Spence, J. T. *Inorg. Chem.* **1982**, *21*, 1602.

(20) Taylor, R. D.; Todd, P. G.; Chasteen, N. D.; Spence, J. T. *Inorg. Chem.* **1979**, *8*, 44.

(21) Scullane, M. I.; Taylor, R. D.; Minelli, M.; Spence, J. T.; Yamanouchi, K.; Enemark, J. H.; Chasteen, N. D. *Inorg. Chem.* **1979**, *18*, 3213.

and hence does not interact with the ^{14}N nuclei.

The EPR spectrum for $[Et_4N][Mo(hbma)_2]$ is apparently axial. It is possible there is some anisotropy in $g_\perp$, which is too small to be detected at X-band frequencies but which would be evident at Q-band frequencies.[21] However, it has been shown for some Cu(II) and VO^{2+} complexes that magnetic symmetry does not necessarily imply structural symmetry.[22] Small changes in ligand field strength can produce large changes in EPR spectra, which may account for the differences between the EPR spectra of $[Et_4N][Mo(hbma)]$ (axial) and $[Mo(hbha)]^-$ (rhombic).[22] Complete assignments of the EPR spectra of these Mo(V) complexes would require oriented crystal EPR experiments.

The EPR parameters for the Mo(V)–oxo complexes with mae^{4-}, mab^{4-}, and $hbpd^{4-}$ indicate $A_z > A_x, A_y$, which is the general pattern for Mo(V)–oxo complexes.[21] Since the structure of $[MoO(hae)]^-$ is expected to be similar to that of the other Mo(V)–oxo complexes, the reason for $A_x > A_y, A_z$ is not evident. In this regard, structures of the complexes would be most helpful. Unfortunately, attempts to grow suitable crystals of $[Et_4N][MoO(mab)]$ and $[Et_4N][MoO(mae)]$ for X-ray structure analysis have not been successful; likewise, repeated attempts using a variety of methods and a number of cations to obtain solid complexes giving satisfactory analyses for $[MoO(hbpd)]^-$ and $[MoO(hae)]^-$ have failed.

The results demonstrate the ability of high-oxidation-state (+6, +5) Mo to deprotonate aromatic amino ligands. While the results with N_2S_2 and NOS donor sets are not surprising, the ability to deprotonate amino groups in N_2O_2 and NO_2 donor sets is unexpected; no complexes with ligands having aromatic oxygen donors that exhibit this behavior have been reported.[7] Furthermore, the formation of Mo(V)–oxo complexes with deprotonated amino ligands is also unexpected, considering the π-donor strength of oxygen. The properties and structures of such complexes clearly represent a balance between oxidation state and π donation by oxygen. The corresponding Mo(VI)–dioxo complexes are normal (i.e., protonated amino groups), and it might be expected the corresponding Mo(IV)–oxo complexes would also be normal because of the lower oxidation state of Mo. The cyclic voltammograms for one-eletron reduction of the Mo(V)–oxo complexes, however, are reversible, indicating simple electron transfer without ligand modification, and quantitative one-electron reduction by controlled-potential coulometry of $[Et_4N][MoO(mae)]$ and $[Et_4N][MoO(mab)]$ gives solutions having identical cyclic voltammograms as for the Mo(V)–oxo complexes.[8]

The relation between structure and ^{14}N shfs of the Mo(V) EPR signal of the complexes is of some interest. The well-resolved ^{14}N shfs of $\sim 2 \times 10^{-4}$ cm^{-1} for two equivalent N atoms, observed with the Mo(V)–oxo complexes, requires considerable overlap of π orbitals on trigonal N with the d_{xy} orbital of Mo (orthogonal to the Mo=O bond). With the non-oxo complexes, however, no ^{14}N shfs is seen, indicating minimum overlap of the N π orbital and the Mo d orbital containing the unpaired electron and suggesting the N atoms are not in the plane of the d orbital containing the unpaired electron.

Experimental Section

Materials. Reagent grade solvents, distilled and dried by standard methods, were used in all cases. Solutions were deaerated with 99.997% N_2.

o-(Salicylideneamino)phenol was purchased from Pfaltz and Bauer. Salicylaldehyde 2-mercaptoanil was prepared by the method of Muto.[23] $^{98}MoO_3$ (97.23% ^{98}Mo) was purchased from Oak Ridge National Laboratory. $MoO_2(acac)_2$ and $^{98}MoO_2(acac)_2$ were prepared by the method of Rajan and Chakravorty.[24] $[Et_4N][MoO(SC_6H_4CH_3)_4]$ and $[Et_4N][MoO(SC_6H_5)_4]$ were prepared as described by Boyd et al.[25]

Syntheses. Ligands. The Schiff basses of the ligands $hbmaH_3$, $hbhaH_3$, $hbpdH_4$ were prepared as described by Corbin and Work for similar ligands.[26a] The Schiff base of $haeH_3$ was obtained by the method of Bayer.[26b] The Zn^{2+} salts of the ligands $maeH_2^{2-}$ and $mabH_2^{2-}$ and the free ligands $maeH_4$, $mabH_4$, and $haeH_4$ were prepared by the method of Corbin and Work.[26a] The crude yield of $haeH_4$ was 65%, and recrystallization gave a 45% yield of product.

$hbmaH_3$ and $hbhaH_3$. The Zn^{2+} salt of the Schiff base of the ligands (6.0 g) was added in small amounts to a stirred solution (1.50 g) of $LiAlH_4$ in 200 mL of dry THF. After addition was complete, stirring was continued for 1 h. The solution was warmed to 60 °C and stirred for an additional 1 h. Excess $LiAlH_4$ was destroyed by slow addition of a 1:1 THF–H_2O mixture. After addition of 25.0 mL of 2 N NaOH, the mixture was stirred at 60 °C for 45 min. It was then acidified with 0.05 N H_2SO_4. The THF layer was separated and the solvent removed in a rotary evaporator. The product was extracted into $CHCl_3$ and the $CHCl_3$ dried over Na_2SO_4. A thick, yellow, oily liquid was obtained by removal of $CHCl_3$ in a rotary evaporator, giving 1.5 g of ligand in both cases (28% and 30% yields, respectively).

$Zn(hbpH_2)$. A solution of 5.0 g of the Zn^{2+} salt of the Schiff base of $hbpH_2^{2-}$ in 40.0 mL of dry DMF was added to 20.0 mL of dry MeOH, and the mixture was deaerated and cooled in an ice bath. To this cooled solution was added with stirring 0.20 g of $NaBH_4$ in small amounts over a period of 40 min. The solution was stirred for 1 h while cold and then overnight at room temperature. The resulting light orange solution was filtered, and 200 mL of deaerated H_2O was added, giving a light yellow precipitate. The solid was filtered off and dried at 30 °C under vacuum, giving 2.0 g (40% yield) of product.

Complexes. $Mo(hbma)_2$. A solution of 0.46 g (2.0 mmol) of $hbmaH_3$ in MeOH (30.0 mL) was added to 0.65 g (2.0 mmol) of $MoO_2(acac)_2$ in 30.0 mL of CH_3OH. The resulting red-brown solution was warmed with stirring until a green solid precipitated. The solid was filtered off, washed with MeOH, and dried at 30 °C under vacuum. Anal. Calcd for $MoC_{26}H_{20}N_2O_2S_2$: C, 56.52; H, 3.65; N, 5.07; S, 11.59. Found: C, 56.08; H, 3.85; N, 4.89; S, 11.26.

$Mo(hbha)_2$. A solution of 0.80 g (2.4 mmol) of $MoO_2(acac)_2$ in MeOH (30.0 mL) was added to 0.43 g (1.8 mmol) of $hbhaH_3$ in 40.0 mL of MeOH. The resulting red-brown solution was filtered and warmed to 60 °C with stirring. A green-brown precipitate formed and was separated by filtration, washed with MeOH, and dried at room temperature under vacuum. Anal. Calcd for $MoC_{26}H_{20}N_2O_4$: C, 60.00; H, 3.87; N, 5.38. Found: C, 59.83; H, 4.02; N, 5.12.

$^{98}Mo(hbma)_2$ and $^{98}Mo(hbha)_2$. These complexes were prepared from $^{98}MoO_2(acac)_2$, obtained from $^{98}MoO_3$, as described above.

$[Et_4N][Mo(hbma)_2]$. A solution of 0.74 g (1.0 mmol) of $[Et_4N][MoO(CH_3C_6H_4S)_4]$ in 20.0 mL of dry, aerated MeCN was slowly added to a deaerated solution of 0.20 g (2.0 mmol) of Et_3N and 0.40 g (1.7 mmol) of $hbmaH_3$ in 30.0 mL of dry, deaerated EtOH. The solution was heated to 70–80 °C for 40 min. Upon slow cooling, dark green-brown crystals were formed, which were filtered off, washed with a dry, deaerated EtOH–Et_2O (1:1) mixture, and dried at room temperature under vacuum. A few crystals were selected for X-ray analysis. Anal. Calcd for $MoC_{34}H_{40}N_3O_2S_2$: C, 59.81; H, 5.90; N, 6.15; S, 9.39. Found: C, 59.64; H, 5.88; N, 5.99; S, 9.15.

$MoO_2(hbpdH_2)$. A solution of 0.77 g (2.0 mmol) of $Zn(hbpdH_2)$ in 30.0 mL of MeOH was added slowly to 0.65 g (2.0 mmol) of $MoO_2(acac)_2$ in 30.0 mL of MeCN. The resulting brown solution was filtered and the volume reduced under vacuum with warming. Upon cooling, a yellow solid precipitated. This was filtered off, washed with cold MeCN, and dried at room temperature under vacuum. Anal. Calcd for $MoC_{20}H_{18}N_2O_4$: C, 53.81; H, 4.06; N, 6.27. Found: C, 51.53; H, 4.41; N, 5.97.

$MoO_2(maeH_2)$ and $MoO_2(mabH_2)$. These complexes were prepared by the method of Gardner et al.,[5,6] as modified by Minelli,[27] from

(22) (a) Hitchman, M. A.; Olson, C. D.; Belford, R. L. *J. Chem. Phys.* **1969**, *50*, 1195. (b) Belford, R. L.; Pilbrow, J. R. *J. Magn. Reson.* **1973**, *11*, 381. (c) Belford, R. L.; Harrowfield, B.; Pilbrow, J. R. *Ibid.* **1977**, *28*, 433.

(23) Muto, Y. *Bull. Chem. Soc. Jpn.* **1960**, *33*, 1242.

(24) Rajan, O. A.; Chakravorty, A. *Inorg. Chem.* **1981**, *20*, 660.

(25) Boyd, I. W.; Dance, J. G.; Landers, A. E.; Wedd, A. G. *Inorg. Chem.* **1979**, *18*, 1875.

(26) (a) Corbin, J. L.; Work, D. E. *Can. J. Chem.* **1974**, *52*, 1054. (b) Bayer, E. *Chem. Ber.* **1957**, *90*, 2325.

the free ligand $maeH_4$ and the Zn^{2+} salt of $mabH_2^{2-}$, respectively.

MoO_2(haeH$_2$). This complex was prepared by the method of Gardner, et al.,[5b] as modified by Minelli,[27] from the free ligand $haeH_4$ as described for the corresponding amino thiol. Anal. Calcd for $MoC_{14}H_{14}N_2O_4$: C, 45.42; H, 3.81; N. 7.57. Found: C, 45.69; H, 3.70; N, 7.79.

[Et$_4$N][MoO(mae)]. To a solution of 0.25 g (0.75 mmol) of Zn(maeH$_2$) in 100 mL of dry, aerated CH_2Cl_2 were added 0.50 g (3.0 mmol) of [Et$_4$N]Cl and 0.50 g (0.74 mmol) of [Et$_4$N][MoO(SC$_6$H$_5$)$_4$]. The solution was warmed at 30–40 °C until a green color developed, and a green solid precipitated. The solid was filtered off and dried under vacuum at room temperature. This complex is unstable toward O_2 and must be stored in an ampule under vacuum in the refrigerator. Anal. Calcd for $MoC_{22}H_{32}N_3OS_2$: C, 51,35; H, 6.28; N, 8.17; S, 12.46. Found: C, 51.02; H, 6.10; N, 7.89; S, 12.13.

[Et$_4$N][MoO(mab)]. To a solution of 0.21 g (0.72 mmol) of $mabH_4$ in 40.0 mL of dry, deaerated MeCN were added 1.0 g (6.0 mmol) of [Et$_4$N]Cl andd 0.47 g (0.70 mmol) of [Et$_4$N][MoO(SC$_6$H$_5$)$_4$]. The solution was warmed at 60 °C until a green color developed; 40.0 mL of dry deaerated MeOH was then added and the solution cooled in an ice bath for 60 min. A dark green precipitate formed, which was collected and dried under vacuum at room temperature. This complex is also unstable to O_2 and must be stored under vacuum in a sealed ampule in the refrigerator. Anal. Calcd for $MoC_{24}H_{36}N_3OS_2$: C, 53.12; H, 6.70; N, 7.75; S, 11.82. Found: C, 53.21; H, 6.45; N, 7.48; S, 11.64.

IR and ^{1}H NMR spectra of the ligands and IR spectra of the complexes were routinely obtained and used to identify expected features of products.

Electrochemistry. Cyclic voltammetry and coulometry were performed in DMF, MeCN (Burdick and Jackson, dried over Linde AW-500 sieves), and CH_2Cl_2 (distilled, dried) with [Et$_4$N]Cl or [n-Bu$_4$N][BF$_4$] as electrolyte, with use of a three-electrode cell described previously[28] and a PAR Model 173 potentiostat, Model 174 polarographic analyzer, and Model 175 signal generator. Potential measurements (E_p, E_c, $E_{1/2}$) have a precision of ±0.005 V, and number of electrons (n) are the averages of duplicate runs with a precision of ±0.10 electron/molecule.

EPR. EPR spectra were obtained with a Varian E-109 spectrometer. Samples were prepared under N_2, transferred to EPR tubes with gas-tight syringes, and frozen immediately in liquid N_2. Spectra at other temperatures were obtained with use of an evacuated flat cell and a variable-temperature accessory.

EPR parameters were obtained by best fit simulations using a program developed by White and Belford[29] and modified by White et al.,[30] obtained from N. D. Chasteen, Department of Chemistry, University of New Hampshire. The program has provision for noncoincidence of **g** and **A** tensors; simulations using various angles of noncoincidence, however, did not significantly improve the fit for any complex. For accurate determination of noncoincidence angles, simulation at Q-band frequency appears to be necessary.[21] Best fit was determined by visual inspection and a computer program that finds the minimum in the summation of differences between simulated and measured spectra. The EPR spectra of ^{98}Mo(V) complexes with $hbma^{3-}$ and $hbha^{3-}$ were used to obtain the best fit for g values and, by comparison to the naturally occurring isotopic spectra, to identify features arising from ^{95,97}Mo coupling.

Estimates of spin concentrations, using known Mo(V) complexes as standards ($K_3Mo(CN)_8$, MoOCl(thiooxine)$_2$),[13] indicated the Mo(V) complexes reported are 100 ± 10% EPR active.

X-ray Structure Determination of [Et$_4$N][Mo(hbma)$_2$]. The structure of [Et$_4$N][Mo(hbma)$_2$] was determined from single-crystal data obtained with a Syntex P2$_1$ autodiffractometer. Crystallographic details are summarized in Table III. The data were reduced to F_o^2 and $\sigma(F_o^2)$ by the procedures previously described.[6a] Lorentz and polarization corrections were made, but an absorption correction was not necessary. All computations were performed on the CDC CY-175 computer at the University of Arizona Computer Center. Details of the programs used in the course of the structure determination are described in a previous paper.[6a] Neutral-atom scattering factors used for the non-hydrogen atoms were obtained from ref 31. The H atom scattering factors were taken from the calculation of Stewart, Davidson, and Simpson.[32]

Table V. Final Atomic Parameters for [Et$_4$N][Mo(hbma)$_2$]

atom	x	y	z	B, Å^2
Mo	0.30083 (6)	0.09812 (6)	−0.09486 (6)	*a*
S1	0.41835 (16)	0.05218 (18)	−0.07077 (17)	*a*
S2	0.30262 (18)	0.18374 (18)	−0.18727 (17)	*a*
O1	0.1930 (4)	0.0957 (4)	−0.1122 (4)	*a*
O2	0.2757 (4)	0.0614 (4)	−0.0031 (4)	*a*
N1	0.3001 (4)	0.0051 (5)	−0.1578 (4)	*a*
N2	0.3396 (4)	0.1948 (5)	−0.0449 (4)	*a*
C1	0.4188 (6)	−0.0285 (6)	−0.1213 (5)	3.38 (23)
C2	0.4793 (6)	−0.0757 (6)	−0.1213 (6)	4.60 (27)
C3	0.4762 (7)	−0.1405 (7)	−0.1610 (6)	5.6 (3)
C4	0.4166 (7)	−0.1595 (7)	−0.2004 (6)	5.6 (3)
C5	0.3563 (6)	−0.1103 (7)	−0.2030 (6)	4.81 (27)
C6	0.3578 (6)	−0.0454 (6)	−0.1626 (5)	3.53 (24)
C7	0.2354 (6)	−0.0051 (6)	−0.2053 (6)	4.18 (27)
C8	0.1720 (6)	−0.0217 (6)	−0.1689 (6)	4.14 (26)
C9	0.1534 (7)	0.0333 (7)	−0.1220 (6)	4.69 (28)
C10	0.0920 (7)	0.0196 (7)	−0.0875 (6)	5.5 (3)
C11	0.0521 (7)	−0.0456 (8)	−0.0991 (6)	6.0 (3)
C12	0.0698 (6)	−0.0992 (8)	−0.1462 (6)	5.59 (27)
C13	0.1302 (6)	−0.0881 (7)	−0.1807 (6)	5.01 (27)
C14	0.3453 (5)	0.2619 (6)	−0.1480 (6)	3.55 (24)
C15	0.3624 (6)	0.3274 (7)	−0.1885 (6)	4.54 (27)
C16	0.3972 (6)	0.3895 (7)	−0.1545 (6)	5.23 (28)
C17	0.4148 (6)	0.3866 (7)	−0.0870 (6)	5.32 (29)
C18	0.3991 (6)	0.3225 (7)	−0.0479 (6)	4.64 (27)
C19	0.3631 (5)	0.2598 (6)	−0.0790 (6)	3.51 (24)
C20	0.3567 (6)	0.1910 (6)	0.0302 (6)	4.53 (27)
C21	0.2948 (6)	0.1693 (6)	0.0664 (6)	4.25 (26)
C22	0.2572 (6)	0.1025 (8)	0.0499 (6)	4.43 (24)
C23	0.1985 (7)	0.0791 (6)	0.0833 (6)	5.16 (29)
C24	0.1813 (7)	0.1222 (7)	0.1383 (7)	5.9 (3)
C25	0.2176 (7)	0.1856 (7)	0.1575 (6)	5.4 (3)
C26	0.2745 (6)	0.2107 (7)	0.1241 (6)	5.4 (3)
N3	0.1304 (5)	0.3352 (5)	−0.0738 (4)	4.18 (20)
C27	0.1223 (6)	0.2786 (7)	−0.1323 (6)	5.00 (28)
C28	0.0487 (8)	0.2768 (8)	−0.1670 (7)	8.3 (4)
C29	0.0801 (6)	0.3182 (6)	−0.0199 (6)	4.48 (26)
C30	0.0889 (7)	0.2390 (8)	0.0073 (7)	7.5 (4)
C31	0.1145 (6)	0.4172 (6)	−0.0962 (5)	4.77 (28)
C32	0.1568 (7)	0.4444 (8)	−0.1522 (7)	7.0 (4)
C33	0.2076 (6)	0.3291 (6)	−0.0440 (6)	4.66 (27)
C34	0.2269 (6)	0.3740 (7)	0.0178 (6)	5.5 (3)

[a] Atom refined anisotropically.

Table VI. Spectroscopic Data

complex	electronic λ max, nm (log ε)	IR[a] $\nu_{Mo=O}$, cm^{-1}
Mo(hbma)$_2$[b]	495 (4.19), 297 (3.94)	
Mo(hbha)$_2$[b]	543 (4.00), 440 (4.26), 270 (4.16)	
MoO_2(haeH$_2$)[c]	322 (3.66)	930, 910
MoO_2(hbpdH$_2$)[d]	498 (2.84), 353 (3.68), 282 (4.14)	915, 887
[Et$_4$N][Mo(hbma)$_2$][b]	610 (3.55), 425 (4.20), 300 (4.18)	
[Mo(hbha)$_2$]$^-$[b]	620 (3.67), 436 (4.15), 353 (4.32)	
[MoO(hae)]$^-$[c]	695 (1.83), 447 (2.97), 319 (4.03)	
[MoO(hbpd)]$^-$[d]	652 (2.56), 492 (3.26), 403 (3.61)	

[a] Solid mull. [b] CH_2Cl_2. [c] DMF. [d] MeCN.

(27) Minelli, M. Dr. Rer. Nat. Dissertation, Universität Konstanz, Konstanz, West Germany, 1980.
(28) Taylor, R. D.; Street, J. P.; Minelli, M.; Spence, J. T. *Inorg. Chem.* **1978**, *17*, 3207.
(29) White, L. K.; Belford, R. L. *J. Am. Chem. Soc.* **1976**, *98*, 4428.
(30) White, L. K.; Albanese, N.; Chasteen, N. D., unpublished work.
(31) "International Tables for X-ray Crystallography"; Kynoch Press: Birmingham, England, 1974; Vol. IV.
(32) Stewart, R. F.; Davison, E. R.; Simpson, W. T. *J. Chem. Phys.* **1965**, *42*, 3175.

The position of the Mo atom was determined by direct methods. All the remaining non-hydrogen atoms were located by structure factor calculations and difference electron density maps. The structure was refined by full-matrix least-square techniques, minimizing the function $\sum w(|F_o| - |F_c|)^2$ with $w = 4F_o^2/[\sigma^2(F_o^2) + (pF_o^2)^2]$, where p was set equal to 0.03. Hydrogen atoms were included as fixed contributions at idealized coordinates in the final cycles of refinement. Refinement of the model with anisotropic thermal parameters for Mo, N1, N2, S1, S2, O1, and O2 resulted in $R_1 = \sum||F_o| - |F_c||/\sum|F_o| = 0.074$ and $R_2 = [\sum w(|F_o| - |F_c|)^2/\sum wF_o^2]^{1/2} = 0.058$. The "goodness of fit" $[\sum w(|F_o| - |F_c|)^2/(n - m)]^{1/2} = 1.569$, where n is the number of data (2355) and m is the number of variables (204). Atomic coordinates are given in Table V; anisotropic thermal parameters and values of $|F_o|$ and $|F_c|$ are available as supplementary data.

Acknowledgment. Financial support of this work by NIH Grants GM08437 (J.T.S.) and ES00966 (J.H.E.) is gratefully acknowledged.

Registry No. $Mo(hbma)_2$, 86953-19-7; $Mo(hbha)_2$, 86942-41-8; $MoO_2(haeH_2)$, 86942-43-0; $MoO_2(hbpdH_2)$, 84214-36-8; $MoO_2(acac)_2$, 17524-05-9; $[Et_4N][MoO(SC_6H_4CH_3)_4]$, 86942-45-2; $[Et_4N][Mo(hbma)_2]$, 86953-21-1; $[Mo(hbha)_2]^-$, 86953-22-2; $[MoO(hae)]^-$, 86953-23-3; $[MoO(hbpd)]^-$, 86942-46-3; $[Et_4N][MoO(mae)]$, 74577-39-2; $[Et_4N][MoO(mab)]$, 74577-41-6; $Zn(hbpH_2)$, 86942-47-4.

Supplementary Material Available: Listings of thermal parameters and structure factors for $[Et_4N][Mo(hbma)_2]$ (11 pages). Ordering information is given on any current masthead page.

Contribution from the Department of Inorganic Chemistry, Free University, 1081 HV Amsterdam, The Netherlands

Proton Exchange in the Base-Catalyzed Ammoniation of the *trans*-Dichlorotetraamminecobalt(III) Cation

SIJBE BALT,* HENDRIKUS J. GAMELKOORN, HENRICUS J. A. M. KUIPERS, and WILLEM E. RENKEMA

Received December 21, 1982

The ammoniation of the *trans*-$[Co(NH_3)_4Cl_2]^+$ cation to $[Co(NH_3)_5Cl]^{2+}$, studied in liquid ammonia between −40 and −60 °C, follows the two-step conjugate-base mechanism and gives over 98% stereochemical retention, as shown by $^{15}NH_3$ labeling. Activation parameters for the overall reaction ($K^{CB}k_2$) are $\Delta H^* = 59$ kJ mol^{-1} and $\Delta S^* = -55$ J K^{-1} mol^{-1}. At ammonium perchlorate concentrations below 0.01 mol kg^{-1} deprotonation is rate determining and exhibits general base catalysis, with NH_3 and NH_2^- as proton-abstracting bases. Activation parameters for the proton abstraction by NH_3 are $\Delta H^* = 57$ kJ mol^{-1} and $\Delta S^* = -62$ J K^{-1} mol^{-1}. ^1H NMR measurements in N^2H_3 during ammoniation revealed the loss of one proton in the formation of the pentaammine. The ratio between the rate constants for dissociative elimination of the chloro ligand and proton reentry via the solvent path has an average value of 88. At high ammonium concentrations (>0.1 mol kg^{-1}) acid-dependent reprotonation becomes faster than the elimination of the chloro ligand, thus reverting the reaction to "normal" behavior, exemplified by a relatively fast proton-transfer preequilibrium.

Introduction

Base-catalyzed hydrolysis of cobalt(III) amine complexes can be explained by the two-step conjugate-base (CB) mechanism, consisting of a fast proton-transfer preequilibrium, followed by a rate-determining dissociative elimination of the leaving group.[1,2] Tobe and co-workers found that base hydrolysis and reprotonation are comparable in rate for a number of complexes of the *trans*-$[CoL_4X_2]^+$ type, where L_4 is a four-nitrogen donor set and X is a halide.[3,4]

Our group has been studying base-catalyzed ammoniation reactions of cobalt(III) and rhodium(III) complexes.[5-10] From the results obtained it seems that up to now at least two complexes of the *trans*-$[CoL_4X_2]^+$ type show limiting behavior in liquid ammonia: the first ammoniation step of the *trans*-[dichloro[(*RS*)-1,9-diamino-3,7-diazanonane]cobalt(III)] cation[10] and of the *trans*-dichlorobis(ethylenediamine)cobalt(III) cation.[7,11]

For liquid ammonia, in contrast to water, the reprotonation reaction is pH dependent. Therefore it should be possible to effect a transition from the limiting (as to proton transfer) to the "normal" case. For the further elucidation of the mechanism of base-catalyzed reactions, we made a search for cobalt(III) complexes showing the behavior indicated. Among a number of *trans*-$[CoL_4X_2]^+$ systems with apparent rate-determining deprotonation, the only compound that satisfies the conditions set out above is the *trans*-$[Co(NH_3)_4Cl_2]^+$ cation.

We present here the medium dependence of the base-catalyzed ammoniation of this compound, together with a definite proof of the role of proton transfer in the mechanism by NMR isotopic techniques.

Experimental Section

Materials. *trans*-$[Co(NH_3)_4Cl_2]Cl$ was prepared from $[Co(NH_3)_4CO_3]_2(SO_4)\cdot 3H_2O$[12] by the Jörgensen method described by Glemser.[13] The perchlorate was prepared by dissolving the chloride

(1) Basolo, F.; Pearson, R. "Mechanisms of Inorganic Reactions", 2nd ed.; Wiley: New York, 1967; p 177.
(2) Tobe, M. L. *Acc. Chem. Res.* **1970**, *3*, 377.
(3) For a survey see: Tobe, M. L., Invited Lecture presented at the 20th International Conference on Coordination Chemistry, India, 1979. Published in "Coordination Chemistry, 20"; Banerjea, D., Ed.; Pergamon Press: Oxford, 1980; p 47.
(4) Ahmed, E.; Tucker, M. L.; Tobe, M. L. *Inorg. Chem.* **1975**, *14*, 1.
(5) Balt, S.; Pothoff, G. F. *J. Coord. Chem.* **1975**, *4*, 167.
(6) Balt, S. *Inorg. Chem.* **1979**, *18*, 133.
(7) Balt, S.; Breman, J.; de Kieviet, W. *J. Inorg. Nucl. Chem.* **1979**, *41*, 331.
(8) Balt, S.; Jelsma, A. *Inorg. Chem.* **1981**, *20*, 733.
(9) Balt, S.; Jelsma, A. *Transition Met. Chem. (Weinheim, Ger.)* **1981**, *6*, 119.
(10) Balt, S.; Renkema, W. E.; van Zijl, P. C. M. *Inorg. Chim. Acta* **1980**, *45*, L241.
(11) We are indebted to Prof. M. L. Tobe for pointing this out to us.
(12) Deutsch, J. L.; Jonassen, H. B. "Inorganic Syntheses"; McGraw-Hill: New York, 1960; Collect Vol. VI, p 173.

0020-1669/83/1322-3072$01.50/0